FEBS Letters 480 (2000) 106–112 FEBS 24010

Observation of DNA–polymer condensate formation in real time at a molecular level

A.L. Martin[a], M.C. Davies[a], B.J. Rackstraw[b], C.J. Roberts[a,*], S. Stolnik[b], S.J.B. Tendler[a], P.M. Williams[a]

[a] *Laboratory of Biophysics and Surface Analysis, School of Pharmaceutical Sciences, University of Nottingham, Nottingham NG7 2RD, UK*
[b] *Advanced Drug Delivery Group, School of Pharmaceutical Sciences, University of Nottingham, Nottingham NG7 2RD, UK*

Received 31 May 2000; revised 23 July 2000; accepted 25 July 2000

Edited by Giorgio Semenza

Abstract Dynamic real time assembly of toroidal and rod-like DNA condensates has been visualised using atomic force microscopy. Imaging has been conducted in an aqueous environment allowing the visualisation of hydrated, pegylated-polymer DNA condensates undergoing dynamic structural movement and conformational change. A major hurdle in the field of gene delivery is cellular transfection and the subsequent transfer of condensed genetic material to the cell nucleus. An increased understanding of the process of DNA condensation will aid the development and optimisation of gene delivery vectors.

Key words: DNA condensation; Atomic force microscope; Gene delivery; Toroid; Rod; Cationic polymer

1. Introduction

Deoxyribonucleic acid (DNA) is seldom present in vivo in an uncondensed state. Specifically condensed DNA structures are integral to DNA replication, viral transfection, and compaction within sperm heads and nucleosomes. Recently interest in the phenomenon of DNA condensation has been further fuelled by the requirement for controllable DNA condensation in non-viral gene therapy to allow packaging within, and transfection from, gene delivery vehicles. Gene therapy has the potential to treat diseases ranging from inherited genetic disorders to acquired conditions and cancer [1,2].

In order for DNA to achieve densely packed condensed conformations the repulsive forces acting along the phosphate backbone must be overcome. It has been demonstrated that approximately 90% of the electrostatic repulsion between DNA segments must be neutralised to allow condensation to occur [3,4]. Multivalent cations for example, polyamines [5,6], polylysine [7,8] and hexamminecobalt(III) [9,10] have been used to induce condensation in vitro. These studies and others have shown condensed DNA existing as toroidal and rod-like condensates. Polyamines, for example spermidine, are believed to induce condensation in vivo [11].

In order to gain an understanding of the organisation of DNA condensate packing and the dynamics of formation, toroidal structures have been extensively characterised experimentally [4,10,12,13] and theoretically [14,15] in order to elucidate how DNA winds within toroids and any structural intermediates of the folding pathway. Here the atomic force microscope (AFM) is used to image the morphology of DNA–polymer condensates at various stages of the condensation process.

AFM has been utilised in a number of applications in the study of DNA, including the visualisation of dynamic processes [16,17] and indeed looking specifically at systems for DNA delivery [8,18,19]. Importantly AFM holds a major advantage over other ultra-resolution imaging techniques in its ability to operate in a range of environments and to study non-labelled species. This allows the study of native biomolecules in aqueous conditions thereby eliminating the structural artefacts that can be introduced when molecules are dehydrated in the sample preparation procedures required in for example transmission electron microscopy (TEM). The requirement of immobilisation of molecule to substrate does though remain. In this study imaging has been carried out in a controlled aqueous environment allowing DNA–polymer condensates to undergo conformational change in real time. An increased knowledge of such structures will benefit the understanding of the condensation process and facilitate improvement in gene delivery technology.

In this study linear poly(amidoamine)s [20] are used to induce condensation. These are biodegradable materials with low cellular toxicity which interact with plasmid DNA to produce complexes that have demonstrated successful transfection in vitro [21], and hence are promising candidates as non-viral DNA delivery vectors. Here a pegylated poly(amidoamine) has been chosen as it is proposed that the inclusion of a hydrophilic region, for example poly(ethylene glycol) (PEG), may overcome the problems of colloidal stability [22,23] of the DNA–polymer complexes. The steric contribution of PEG may also reduce the potential biocompatibility [24] problems seen with poly(amidoamines) [25] on transferring the system from in vitro to in vivo.

2. Materials and methods

2.1. DNA

Two plasmid samples were used in this study. Unless otherwise stated pBR322 plasmid DNA (4365 base pairs) (Sigma-Aldrich, Poole, UK) was used. The 6 kb plasmid pRSVluc (Cobra Therapeutics, Keele, UK) was also used. Both lyophilised plasmids were diluted

*Corresponding author. Fax: (44)-115-951 5100.
E-mail: clive.roberts@nottingham.ac.uk

Abbreviations: AFM, atomic force microscope; TEM, transmission electron microscopy; PEG, poly(ethylene glycol)

0014-5793/00/$20.00
PII: S0014-5793(00)01894-9

to stock solutions of 20 μg ml^{-1} in water. The choice of plasmid did not affect condensate morphology or behaviour.

2.2. Polymer

A PEG-modified poly(amidoamine), ABA copolymer, molecular weight 28 00 Da, was synthesised and supplied courtesy of Dr F. Bignotti (University of Brescia, Italy) [26]. It was supplied as a freeze-dried solid, and prior to use was dissolved in water to give a solution that when added to the DNA solution an equal volume was required to obtain a 5:1, polymer:DNA ratio in terms of polymer repeating units:DNA nucleotides. All water used was obtained from an ELGA purification system (resistivity 15 MΩ cm) and all buffers were filtered through a 0.2 μm pore size filter, (Sartorius, Göttingen, Germany) prior to use.

2.3. AFM imaging

Condensates were prepared by adding 20 μl of polymer solution (138 μg ml^{-1}) to 20 μl of DNA solution (20 μg ml^{-1}). After 5 min incubation, 20 μl of the resulting solution was deposited onto 1 cm^2 of freshly cleaved mica. Imaging was conducted under 10% w/v phosphate-buffered saline, (PBS, 0.014 M NaCl, 0.001 M phosphate, pH 7.4) which was prepared from tablets (Sigma-Aldrich).

A Nanoscope IIIa Dimension 3000 Scanning Force microscope (Digital Instruments Inc., Santa Barbara, CA, USA) was used throughout. All imaging was conducted in tapping mode, with 512×512 data acquisition at a scan speed of 2 Hz under buffer at ambient conditions. Thin-armed, silicon-nitride, oxide-sharpened, triangular cantilevers (Nanosensors, Germany), were selected, operating at a resonant frequency of approximately 8 kHz. All post-imaging analysis was carried out on Nanoscope software. Background slope was removed using a first or second order polynomial function and images were subjected to a median filter.

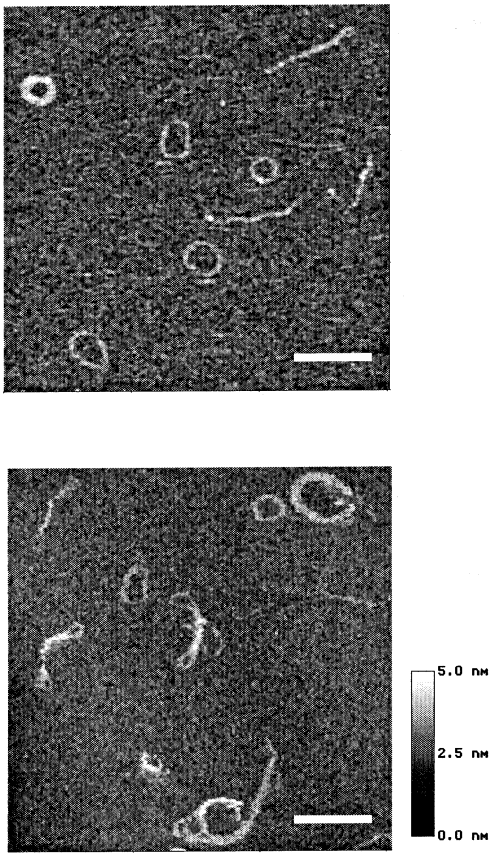

Fig. 1. AFM images of toroidal and rod-like condensates formed with pBR322 and cationic pegylated-poly(amidoamine). All scale bars are equivalent to 300 nm.

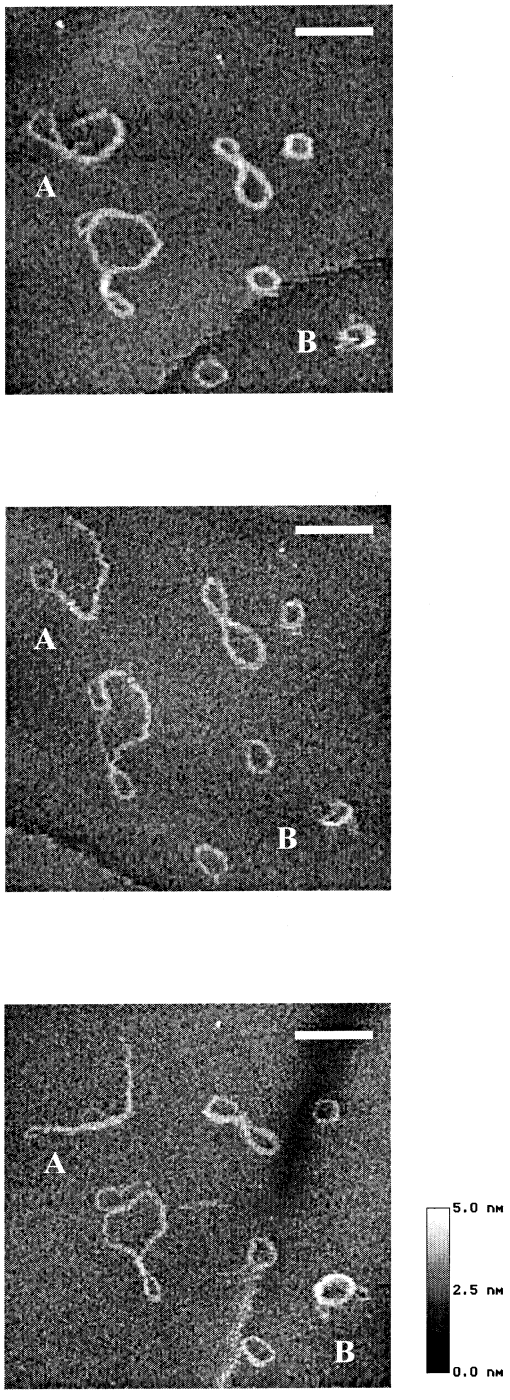

Fig. 2. Real time images of toroidal and rod-like condensates formed with cationic polymer and pBR322. Three consecutive aqueous images acquired at 5 min intervals demonstrating condensate movement in real time. All scale bars are equivalent to 300 nm.

3. Results and discussion

3.1. Formation of DNA–polymer condensates with a cationic polymer

The morphology of uncondensed DNA plasmids has been extensively characterised [27] however when complexed with a cationic polymer the DNA molecules adopt a strikingly different conformation. Toroidal and rod-like or plectonemic condensates are observed, representative images of which are pre-

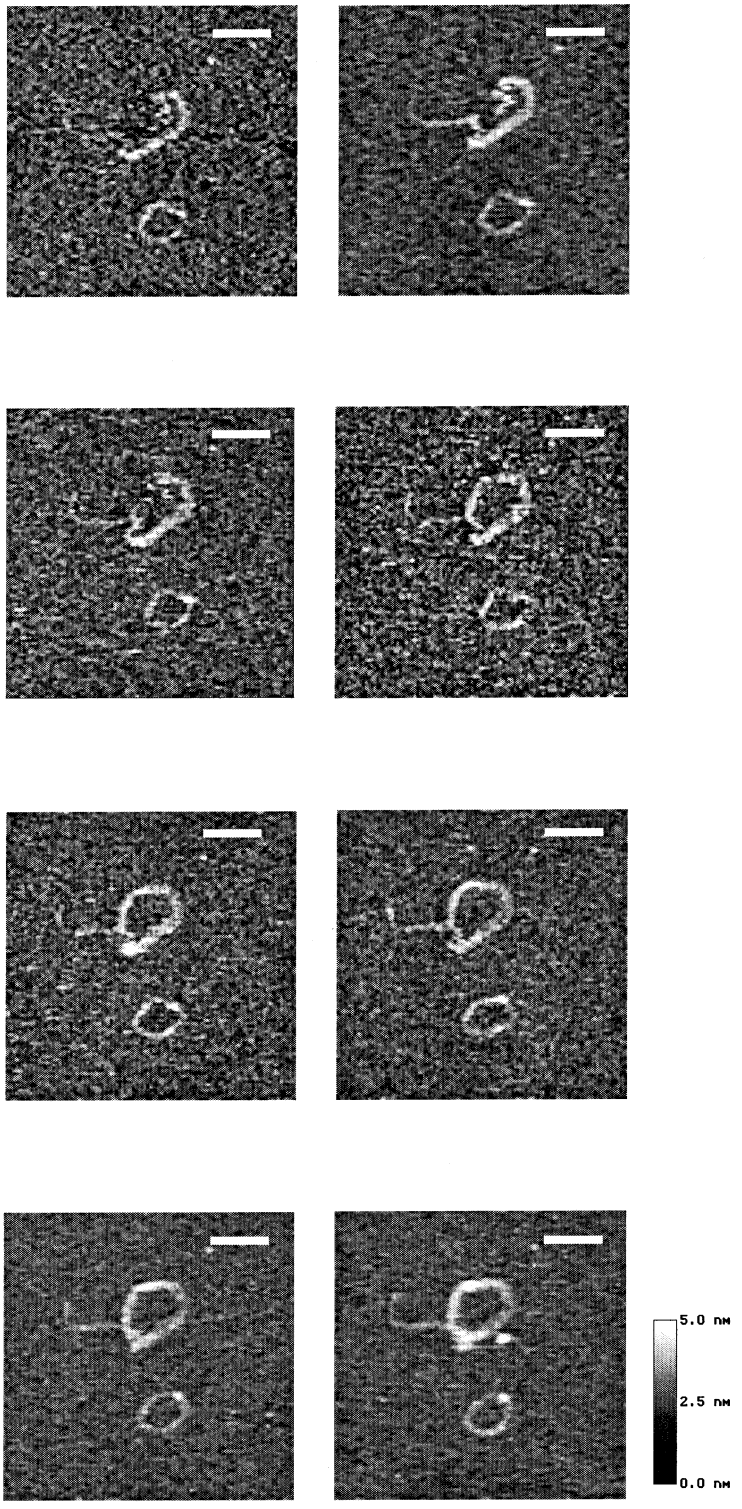

Fig. 3. Real time formation of a toroidal condensate formed with cationic polymer and pBR322. Eight consecutive scans separated by a 5 min time interval showing the formation of a toroidal condensate. Scale bars are equivalent to 200 nm.

sented in Fig. 1. All these condensates have been imaged in an aqueous environment. The morphology of the structures observed is comparable to those reported previously in TEM studies [10,28,29] and theoretically [14,15]. The mean toroidal outer diameter was calculated from four evenly spaced cross-sectional measurements of each molecule. The average outer diameter of 68 toroids was determined to be 133 ± 23 nm. Width measurements were taken at half maximum height in order to minimise the contribution from tip convolution. Toroid outer diameters measured in this study are comparable or slightly larger than those reported elsewhere [10,13,29,30]. This is believed to be due to the hydrated nature of these complexes and to the use of a pegylated-polymer, which is a relatively large molecule with substantial physical presence

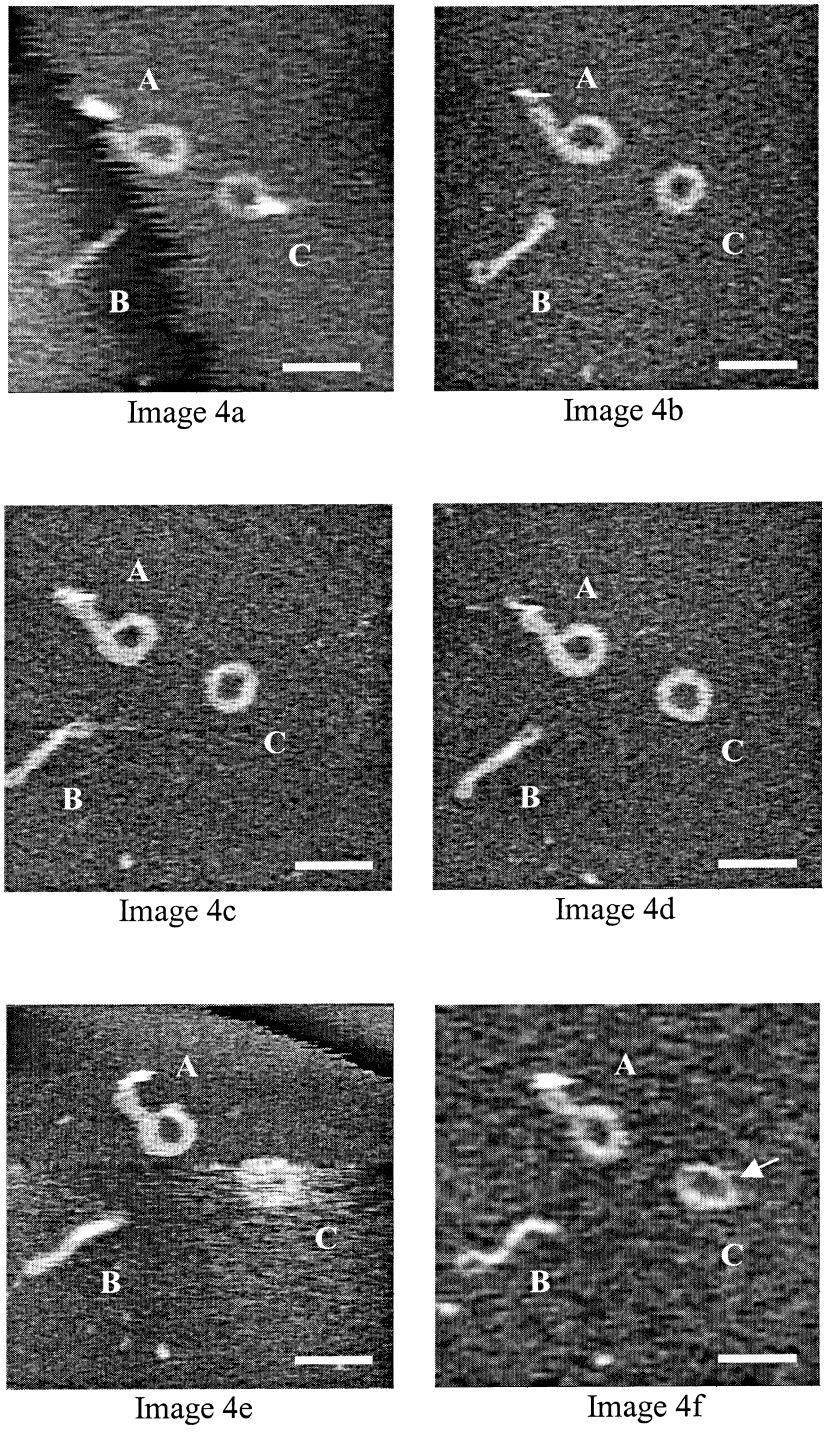

Fig. 4. Aqueous AFM images displaying dynamic equilibrium between toroidal and rod-like condensates. Twelve consecutive images acquired at 5 min time intervals of condensates formed with cationic polymer and plasmid pRSVluc. All scale bars are equivalent to 200 nm.

when compared to a multivalent cation. The variation in toroidal diameter may be due to multimolecular toroidal formation or differing levels of packing density.

Importantly, because immobilisation in this study has been achieved simply on bare mica without substrate modification or the addition of multivalent cations, conformational change has not been induced by immobilisation chemicals [31].

Polymer and DNA have been combined in a 5:1 polymer repeating unit:DNA nucleotide ratio. The excess polymer present is expected to confer a net positive charge upon the condensates. Such positively charged complexes are known to possess higher stability and have higher transfection efficacy, and hence demonstrate more promise in the field of gene delivery [21].

Uncondensed DNA plasmids were never observed on the surface in the presence of polymer. This is due firstly because uncondensed DNA would not be expected to adhere to the untreated, negatively charged mica surface, as it does not possess the net positive charge conferred by the polymer. In addition the polymer is present in a 5:1 excess of the plasmid

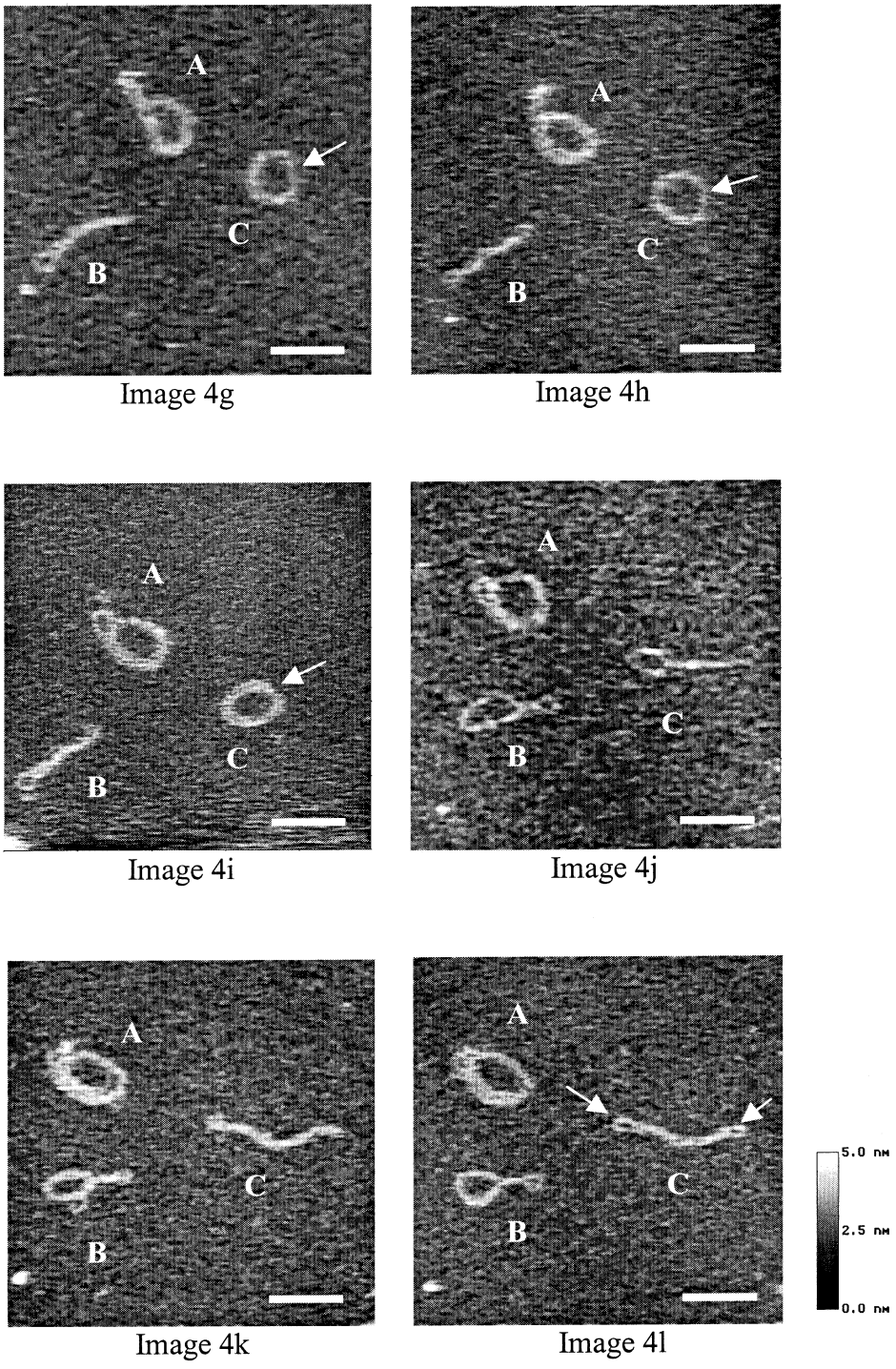

Fig. 4 (*continued*).

so the quantity of uncondensed molecules would be expected to be minimal. Gel electrophoresis of this ratio has also shown the presence of no uncondensed DNA (results not shown).

3.2. Condensate tertiary conformational movement in a liquid environment

AFM has the ability to scan the same surface area repeatedly and hence image dynamic surface changes in real time. Images are generally at time points of a few minutes apart depending on scan size and scan speed, which ultimately depends on the system being studied. In vivo biomolecules are not static entities and undergo conformational movement over time. Fig. 2 shows three consecutive images taken approximately 5 min apart. On close inspection it is observed that over consecutive scans the DNA–polymer condensates undergo tertiary movement. Specific attention is drawn to the plectonemic condensate (A) and the toroidal condensate (B) which both show movement. This movement is not in the scan direction and there is no streaking of the image and hence does not appear to be due to influence of the tip. It is proposed

that although the condensates are immobilised to an extent that allows scanning probe imaging without sweeping the condensates ability to move suggests they are anchored loosely and not irreversibly hence surface immobilisation has been unlikely to induce conformational change in itself.

3.3. Dynamic formation of toroidal and rod-like condensates

An area of focus in the study of DNA condensation is the folding pathway or potential pathways DNA follows in order to form a condensate [10,29,32]. The ability of the AFM to image movement of biomolecules in aqueous conditions provides the opportunity to image the folding process of molecules like DNA as it occurs. Fig. 3 shows eight consecutive images recorded at 5 min intervals. Here the formation of a toroidal like condensate in real time is observed. From such images alone it is not possible to without doubt attribute a model of toroidal formation however, the condensate in Fig. 3 does appear to be forming by fusion of the ends of a curled plectonemic condensate.

When regarding cation-induced DNA condensation an unresolved issue is whether rods are intermediates of toroidal formation or toroids intermediates of rod formation, or indeed whether they are distinct of one another. Fig. 4 shows 12 images at approximately 5 min time intervals, here plasmid pRSVluc was used. Three complexes are observed labelled as shown. First following the progress of complex A, in Fig. 4a it has a 90 nm 'tail' protruding from the top of its structure, over time this becomes less prominent. In Fig. 4i, it is merely a small loop and by Fig. 4l it has coiled into the toroidal-like structure. Complex B, in Fig. 4a this condensate appears as a plectonemic or rod-like structure. Throughout Fig. 4a–i this rod-like structure is maintained however it undergoes slight tertiary movement demonstrating its loose binding to the substrate. In Fig. 4j this rod-like condensate appears to open up and in Fig. 4k,l a ring-like structure develops. Finally attention is drawn to complex C. In Fig. 4a–d this complex possess a toroidal-like morphology. As indicated in Fig. 4f–i a thinner, weaker region on this ring appears to develop. In Fig. 4j the toroidal structure has opened with a rod-like structure being displayed. In Fig. 4l characteristic plectonemic loops are observed at either end of this rod-like structure.

The toroidal structures observed in this system are believed to be fairly loosely wound structures due to the bulky nature of the pegylated-polymer, hence probably represent an early stage of condensate formation. We believe we are observing a stage of condensate formation where ring and rod-like structures exist dynamically, having the ability to reversibly equilibrate between structures.

DNA condensation in vivo is generally regarded as a spontaneous process when electrostatic repulsion of the DNA phosphate backbone is adequately neutralised by cationic molecules [3,4]. The slower speed of condensate formation observed here may be attributed to steric hindrance from the substrate or differences in ionic conditions to that in vivo. Alternatively it is proposed that the use of a relatively large molecular weight polymer with the steric contribution of solvated PEG rather than a small cation may slow down the condensation process. The ability of the partially mica bound complexes to change condensation state allows us to infer that the forces that drive this conformational change are stronger than those that promote binding to the mica. A similar observation was made in the study by Allen et al. [13].

The majority of DNA imaging with AFM has been conducted air [19,30,33] where molecules are dried down on to the substrate effectively fixing the DNA so it is unable to participate in tertiary conformational change. Though this technique is extremely useful in providing snap shots of biomolecular activity it is restricted in that information on process dynamics is limited and structural morphology may contain drying artefacts. DNA morphology is influenced by the ionic concentration of the DNA environment, which is unknown and variable as the sample is dried [34]. Indeed different drying protocols have been shown to alter structural configurations of polycation DNA complexes [8]. There is also the question whether toroidal formation is induced from globular condensates upon evaporation of the solvent [35]. Imaging of biomolecules in liquid offers the ability to elucidate structural conformation without the presence of drying artefacts and observe process dynamics in real time.

In common with all surface imaging there is the question of how closely the composition and morphology of adsorbed structures represents that in the bulk solution. In this study repeated imaging of the sample was possible over a number of hours. Regardless of the duration of imaging no structures were observed other than the rod-like and toroidal condensates already discussed, though the number of condensates on the substrate increased over time as more complexes diffused to the surface. It would be expected that if other structures, for example spherical aggregates, were present then they would adhere to the substrate in a similar manner to the condensates observed.

The data presented here illustrate the ability of the AFM to visualise in situ kinetics of the condensation process and demonstrate its potential role in investigations of the time-resolved mechanics of the condensation process.

4. Conclusions

Atomic force microscopy imaging of DNA and pegylated-polymer complexes in an aqueous environment has been successfully achieved, elucidating toroidal and rod-like condensates. DNA–polymer condensate conformational change has been observed in real time. The morphology and mechanism of condensate assembly has an important place in the development and optimisation of potential gene delivery vectors. The role of AFM in the clarification of these mechanisms has been demonstrated.

References

[1] Ledley, F.D. (1996) Pharm. Res. 13, 1595–1614.
[2] Dachs, G.U., Dougherty, G.J., Stratford, I.J. and Chaplin, D.J. (1997) Oncol. Res. 9, 313–325.
[3] Wilson, R.W. and Bloomfield, V.A. (1979) Biochemistry 18, 2192–2196.
[4] Widom, J. and Baldwin, R.L. (1980) J. Mol. Biol. 144, 431–453.
[5] Gosule, L.C. and Schellman, J.A. (1978) J. Mol. Biol. 121, 311–326.
[6] Allison, S.A., Herr, J.C. and Schurr, J.M. (1981) Biopolymers 20, 469–488.
[7] Shapiro, J.T., Leng, M. and Felsenfeld, G. (1969) Biochemistry 8, 3219–3232.
[8] Hansma, H.G., Golan, R., Hsieh, W., Lollo, C.P., Mullen-Ley, P. and Kwoh, D. (1998) Nucleic Acids Res. 26, 2481–2487.
[9] Widom, J. and Baldwin, R.L. (1983) Biopolymers 22, 1595–1620.
[10] Arscott, P.G., Li, A. and Bloomfield, V.A. (1990) Biopolymers 30, 619–630.

[11] Hung, D.T., Marton, L.J., Deen, D.F. and Shafer, R.H. (1983) Science 221, 368–370.
[12] Schellman, J.A. and Parthasarathy, N. (1984) J. Mol. Biol. 175, 313–329.
[13] Allen, M.J., Bradbury, E.M. and Balhorn, R. (1997) Nucleic Acids Res. 25, 2221–2226.
[14] Hud, N.V., Downing, K.H. and Balhorn, R. (1995) Proc. Natl. Acad. Sci. USA 92, 3581–3585.
[15] Noguchi, H., Saito, S., Kidoaki, S. and Yoshikawa, K. (1996) Chem. Phys. Lett. 261, 527–533.
[16] Guthold, M., Bezanilla, M., Erie, D.A., Jenkins, B., Hansma, H.G. and Bustamante, C. (1994) Proc. Natl. Acad. Sci. USA 94, 12927–12931.
[17] Kasas, S. et al. (1997) Biochemistry 36, 461–468.
[18] Dunlap, D.D., Maggi, A., Soria, M.R. and Monaco, L. (1997) Nucleic Acids Res. 25, 3095–3101.
[19] Fang, Y. and Hoh, J.H. (1998) J. Am. Chem. Soc. 120, 8903–8909.
[20] Ranucci, E., Spagnoli, G., Ferruti, P., Sgouras, D. and Duncan, R. (1991) J. Biomater. Sci. Polym., 2nd edn.
[21] Hill, I.R.C., Garnett, M.C., Bignotti, F. and Davis, S.S. (1999) Biochim. Biophys. Acta 1427, 161–174.
[22] Stolnik, S. et al. (1994) Pharm. Res. 11, 1800–1808.
[23] Gref, R., Minamitake, Y., Peracchia, M.T., Trubetskoy, V., Torchilin, V. and Langer, R. (1994) Science 263, 1600–1603.
[24] Fuertges, F. and Abuchowski, A. (1990) J. Control. Release 11, 139–148.
[25] Plank, C., Mechtler, K., Szoka, F.C. and Wagner, E. (1996) Hum. Gene Ther. 7, 1437–1446.
[26] Ranucci, E. and Ferruti, P. (1991) Macromolecules 24, 3747–3752.
[27] Pope, L.H., Davies, M.C., Laughton, C.A., Roberts, C.J., Tendler, S.J.B. and Williams, P.M. (1999) Anal. Chim. Acta 400, 27–32.
[28] Plum, G.E., Arscott, P.G. and Bloomfield, V.A. (1990) Biopolymers 30, 631–643.
[29] Böttcher, C., Endisch, C., Fuhrhop, J., Catterall, C. and Eaton, M. (1998) J. Am. Chem. Soc. 120, 12–17.
[30] Lin, Z., Wang, C., Feng, X., Liu, M., Li, J. and Bai, C. (1998) Nucleic Acids Res. 26, 3228–3234.
[31] Fang, Y. and Hoh, J.H. (1998) Nucleic Acids Res. 26, 588–593.
[32] Fang, Y. and Hoh, J.H. (1999) FEBS Lett. 459, 173–176.
[33] Golan, R., Pietrasanta, L.I., Hsieh, W. and Hansma, H.G. (1999) Biochemistry 38, 14069–14076.
[34] Schlick, T., Li, B. and Olson, W.K. (1994) Biophys. J. 67, 2146–2166.
[35] Sergeyev, V.G., Pyshkina, O.A., Lezov, A.V., Mel'nikov, A.B., Ryumtsev, E.I., Zezin, A.B. and Kabanov, V.A. (1999) Langmuir 15, 4434–4440.